

# microRNAs may sharpen spatial expression patterns

Erel Levine\*,<sup>1</sup> Peter McHale\*,<sup>1</sup> and Herbert Levine<sup>†1</sup>

<sup>1</sup>Center for Theoretical Biological Physics, University of California at San Diego, La Jolla, CA 92093

microRNAs (miRNAs) form a ubiquitous class of small RNAs that silence target genes. Surprisingly, in many cases miRNA deletion has no dramatic phenotypic effect. Indeed, miRNAs acting in morphogenetic pathways may fine tune, rather than set up, their targets' expression patterns. Here, we construct a model in which the spatial expression pattern of a target gene, crudely established by a morphogen, is fine-tuned by a cognate miRNA. This is done by generating a sharp interface between domains of high and negligible target expression, thereby unambiguously defining the identity of each cell. The ability of miRNAs to move between cells is crucial to this sharpening. We examine the model in a context where the spatial transcription profiles of miRNA and target are mutually exclusive as, for example, is the case for some Hox genes in the early *Drosophila* embryo. We further consider an alternative scenario, where the two transcription profiles are approximately the same. We show that miRNAs can still sharpen the target expression pattern provided they become irreversibly localized to a cell before interacting with their targets. An experimental test of the proposed mechanism is suggested.

Morphogenesis proceeds by sequential divisions of a developing embryo into regions, each expressing a distinct set of genes. To each combination of genes is associated a particular cell identity. A crucial step in setting the boundaries of these expression patterns is often the establishment of a concentration gradient of molecules called morphogens. Some morphogens are transcription factors which regulate gene expression directly [1, 2]. Others are ligands that bind cell-surface receptors signaling the activation of target expression [3]. Since morphogens act in a concentration-dependent manner, a morphogen gradient is transformed into a gradient of its target messenger RNA (mRNA). At advanced stages of development this spatial mRNA profile is bimodal with an interface between domains of high and low target expression. The interface must be sharp in order to unambiguously define the identity of a cell. A single morphogen interacting cooperatively with its target can in principle generate a sharp interface in the target transcription profile, viz. the rate of mRNA transcription as a function of the nuclear spatial coordinate [4]. This may be done e.g. by cooperative binding to a receptor or to a promoter [5] or by zero-order ultrasensitivity [6]. An obvious limitation in this mechanism is the need for large cooperativity factors. This raises the question of whether other developmental regulators can aid a morphogen gradient in establishing a narrow interface between on and off target-gene expression.

microRNAs (miRNA) constitute a new class of gene regulators that silence their targets by binding to target mRNAs. In metazoans primary miRNA transcripts are transcribed and then processed both inside and outside of the nucleus to form mature transcripts approximately 21

nt in length that are then loaded into the RNA-induced silencing complex (RISC) [7]. They are found in plants [8] and animals [9], including human [10], and are predicted to target a large fraction of all animal protein-coding genes [10, 11, 12]. In plants miRNAs are known to affect morphology [13, 14, 15] implying that they play an important role in determining cell identity. This is underscored by the fact that the spatiotemporal accumulation of miRNAs is under tight control in plants [16], fly [17, 18] and zebrafish [19].

In this study we formulate a mathematical model in which miRNAs help morphogens to determine cell identity by sharpening morphogen-induced expression patterns. Two key ingredients of the model are a miRNA-mRNA interaction describable by mutual annihilation and miRNA intercellular mobility. Within this framework miRNAs generate a sharp interface between those cells expressing high levels of the target mRNA and those expressing negligible levels of mRNA. We use physical arguments to understand the range of parameters where this sharpening occurs. A consequence of our model is that a local perturbation to the transcription profiles can induce a nonlocal effect on the mRNA concentration profile; we outline an experiment to detect this nonlocal property. Finally we consider the special case where the miRNA and target transcription profiles coincide [20]. We show that miRNA preserve their sharpening function provided mobile miRNA change irreversibly to an immobile state before interacting with their targets. By separating mobility and interaction in this way, the target is rescued from miRNA-mediated silencing in selected cells thereby generating a sharp expression pattern.

\*These authors contributed equally to this work.

<sup>†</sup>To whom correspondence should be addressed; e-mail: hlevine@ucsd.edu.

## MODEL AND RESULTS

### Formulation of model from available biological evidence

Our theory comprises three central elements. First, we assume that the miRNA and its target are transcribed in a space-dependent manner. Second, we model the interaction between miRNA and target as an imperfect annihilation reaction. Last, we allow for the possibility that miRNA move between cells. Before defining the model, let us review the available data regarding each of these processes.

microRNAs and their targets are often expressed in a coordinated manner [21]. In many cases (A), the regulatory network is designed to express the miRNA and its targets in a mutually exclusive fashion. For example, the expression patterns of the miRNA miR-196 and its target Hoxb8 are largely nonoverlapping in mouse [20] and chick [22]. Similarly, the nascent transcripts of Ubx, still attached to the DNA, are expressed in a stripe near the center of the early embryo, while nascent iab-4 is simultaneously observed in nuclei posterior to this domain [23]. A recent large-scale study in fly showed that miRNAs and their target genes are preferentially expressed in neighboring tissues [24]. Likewise, in mouse [25] and in human [26], predicted miRNA targets were found at lower levels in tissue expressing the cognate miRNA than in other tissues.

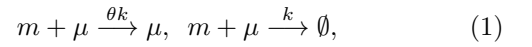
Other typical cases (B) are characterized by co-transcription of the miRNA and its targets [21], as occurs for example in mouse cardiogenesis [27] and human cell proliferation [28]. Likewise, microRNAs encoded within the Hox gene cluster may target co-expressed Hox genes [20].

Our model assumes that the synthesis rate of the miRNA and its target are *smoothly* varying along a spatial axis,  $x$ . This, for example, may be the result of a common morphogen regulating (either directly or indirectly) the two species. The transcription profiles  $\alpha_\mu(x)$  and  $\alpha_m(x)$  of the miRNA and its target, resp., may be anti-correlated (Case A above) or highly correlated (Case B).

The detailed interaction between miRNA and their targets is currently a topic of intense investigation [29, 30]. miRNAs induce the formation of a ribonucleoprotein complex (RISC). Targeting of a specific mRNA by a RISC is done via (often imperfect) base-pair complementarity to the miRNA [9]. Upon binding, protein synthesis is suppressed by either translation inhibition or mRNA destabilization [29, 30]. While it is likely that miRNA can go through a few cycles of mRNA binding [31], the increased endonucleolytic activity conferred by the miRNA makes it plausible that the miRNA is sometimes degraded in the process. In addition, evidence suggests that mRNAs which are translationally repressed by

miRNA are localized to cytoplasmic foci called P-bodies [29, 30, 32]. Taken together, these facts make it improbable that miRNAs act in a fully enzymatic manner.

A pair of mRNA-miRNA reactions that describe a spectrum of plausible scenarios is



where  $m$  represents the mRNA concentration and  $\mu$  represents that of the miRNA. Here,  $\theta$  is the average number of targets degraded by a given miRNA before it is itself lost in the process. These reactions cover the case where the two species reversibly form a complex that is then subject to degradation. This complex may be translationally inhibited. The mutual annihilation reaction also covers the case where the species irreversibly associate. It is a good approximation if the reaction between the species is reversible, provided the typical dissociation time is much longer than the relevant biological time scale. One way in which the cell may control this rate is by regulating exit of the RNA pairs from P-bodies [33].

Can miRNAs move from cell to cell? siRNAs, another important class of small RNAs, are known to illicit non cell autonomous RNA silencing in plants, worms, fly and possibly mouse (reviewed in [34]). Evidence in favor of intercellular mobility of miRNA is found in pumpkin. There, miRNAs have been found in the phloem sap which is transported throughout the plant by phloem tissue [35]. Further suggestive evidence comes from the plant miRNAs mir-165 and mir-166, the distribution of which is consistent with that of a mobile signal [8, 14, 15, 36]. Despite the tentative evidence in favor of miRNA mobility in plants, intercellular transport of miRNA in animals has not yet been observed.

In our model we allow for the possibility that miRNA migrate from cell to cell. Mobility of the miRNA species is likely to rely on active export from the cell followed by import to neighboring cells, or perhaps on direct transport between cells. On the tissue scale, these transport processes are expected to result in effective diffusion. We therefore ignore the small-scale transport processes and model miRNA mobility as pure diffusion.

Finally, we combine these processes into a steady-state mean-field model given by

$$0 = \alpha_m - \beta_m m - k m \mu \quad (2a)$$

$$0 = \alpha_\mu - \beta_\mu \mu - k m \mu + D \mu'' \quad (2b)$$

The  $\beta$  terms describe a linear decay channel for each RNA species and the  $k$  term (mutual annihilation) describes a coupled nonlinear decay channel. Note that the case  $\theta \neq 0$  (imperfect miRNA annihilation) can be brought into this form by renormalizing (2a). The spatial coordinate  $x$  measures distance along one dimension of a tissue of size  $L$ . All our numerical results shall be presented in units of  $L$ , i.e.  $0 \leq x \leq 1$ .

## Sharpening the target expression pattern

In this section we develop a physical understanding of these dynamics in the context of mutually exclusive miRNA ( $\alpha_\mu(x)$ ) and mRNA ( $\alpha_m(x)$ ) transcription profiles (see Fig. 1(a)).

It is instructive to consider first the system in the absence of miRNA diffusion. We make the critical assumption that at any cellular position the decay of the minority species is dominated by the nonlinear channel; by rescaling Eqs. (2) this condition amounts to

$$\max \left\{ \frac{k\alpha_m(x)/\beta_m}{\beta_\mu}, \frac{k\alpha_\mu(x)/\beta_\mu}{\beta_m} \right\} \gg 1, \text{ for all } x. \quad (3)$$

The exact solution of Eqs. (2), with  $D = 0$ , is presented in Fig. 1(a). It can be shown that the steady-state mRNA level is given approximately by

$$m \approx \frac{[\alpha_m - \alpha_\mu]_+}{\beta_m}, \quad (4)$$

where  $[x]_+ = \max\{0, x\}$ . In other words the mRNA level is vanishingly small to the right of the crossing point  $x_e$  of the two transcription profiles. The point  $x_e$  is assumed to reside away from the boundaries. This threshold response in the target profile has been observed in the context of small RNAs—another class of post-transcriptional regulators—in bacteria [37]. In the case of eukaryotic miRNAs this threshold provides insurance against the possibility that the mRNA transcription profile is not as step-like as is required for correct cell differentiation. In other words miRNA regulation is a failsafe mechanism whereby incorrectly transcribed low-abundance transcripts in the region  $x > x_e$  are silenced, while correctly transcribed high-abundance transcripts in the region  $x < x_e$  are only mildly affected [21, 24].

Keeping the large-annihilation-rate limit, Eq. (3), we now introduce diffusion of the miRNA. One expects that diffusion makes the miRNA profile more homogeneous and this is confirmed by exact solutions of the model as shown in Fig. 1(b). The mRNA profile however does not become smoother. In fact exact numerical solutions reveal that there is now a sharper drop from high to low mRNA levels than there was in the absence of diffusion (Fig. 1(c)). More specifically, miRNA diffusion creates an interface between high and negligible target expression. Increasing diffusion moves the interface deeper into the mRNA-rich region and thereby accentuates the drop in mRNA level across the interface (Fig. 1(c)). Two length scales appear in the system and act in concert to obtain this sharp interface. In the miRNA-rich region, at the right end of the developing field, miRNA decay mainly via the linear channel giving rise to the larger length scale  $\lambda$ . In the mRNA-rich region, on the left, miRNA decay mainly via the nonlinear channel resulting in a smaller length scale  $\ell$  that sets the width of the interface. Provided  $\ell \ll L$  diffusion actually increases the sharpness of

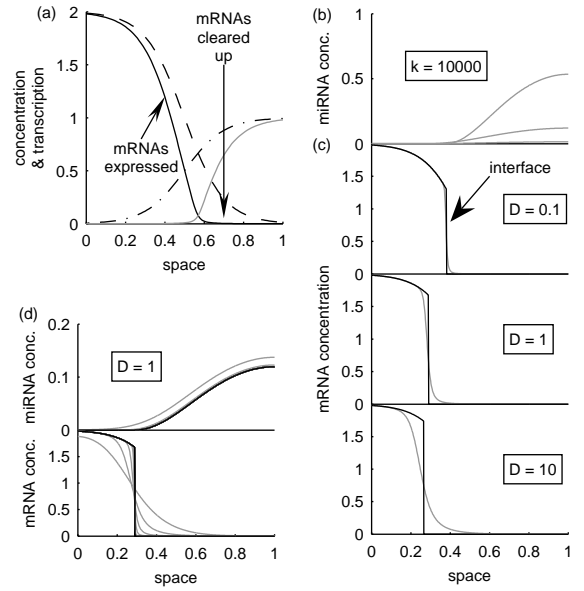


FIG. 1: Sharpening the target expression pattern. Throughout,  $\beta_m = 1$  and  $\beta_\mu = 1$  and the transcription profiles are  $\alpha_m(x) = 0.5A_m[\tanh((x_{tsx}-x)/\lambda_{tsx})+1]$  (dashed line in (a)) and  $\alpha_\mu(x) = 0.5A_\mu[\tanh((x-x_{tsx})/\lambda_{tsx})+1]$  (dashed-dotted in (a)), where  $A_m = 2$ ,  $A_\mu = 1$ ,  $x_{tsx} = 0.5$  and  $\lambda_{tsx} = 0.2$ . (a) In the absence of diffusion miRNAs remove residual mRNAs. mRNA profile in black; miRNA profile in gray. Here  $k = 100$ . (b) Exact miRNA profiles for diffusion constants  $D$  ranging from 0.1 (top) to 10 (bottom) in factors of 10. (c) mRNA profiles corresponding to (b). Analytic solutions in black, exact numerical solutions in gray. (d) miRNA and mRNA profiles for coupling constants  $k$  ranging from  $k = 10^2$  to  $k = 10^6$  in factors of 10. The analytic solution is most accurate at large  $k$ . Note the different scales for the miRNA and mRNA concentrations.

the mRNA profile by shifting the interface towards the mRNA-rich region.

To understand the origin of these length scales consider first the region of space where miRNA are in the majority. In this region, where  $k\mu \gg \beta_m$ , we neglect the linear term in Eq. (2a), yielding  $\alpha_m = km\mu$  and thus

$$0 = \alpha_\mu - \alpha_m - \beta_\mu\mu + D\mu''. \quad (5)$$

Hence miRNA are produced at an effective rate  $\alpha_\mu - \alpha_m$  and diffuse over distances of order

$$\lambda = \sqrt{\frac{D}{\beta_\mu}}, \quad (6)$$

which may be comparable to the system size,  $L$ . On the other hand, in the mRNA-rich zone  $km \gg \beta_\mu$  and so the only length scale available to the miRNA is

$$\ell = \sqrt{\frac{D}{k\alpha_m^*/\beta_m}}, \quad (7)$$

where  $\alpha_m^*$  is a typical value of  $\alpha_m(x)$  in the mRNA-rich zone. For the mRNA this is the only length scale that competes with the spatial layout provided by the transcription profile. When one has  $\ell \ll L$  there is a sharp drop in the mRNA concentration over the only available scale,  $\ell$ . In agreement with the expression in Eq. (7), derived on heuristic grounds, numerical solutions show that the interface width increases with diffusion (Fig. 1(c)) and decreases with annihilation rate (Fig. 1(d)). Since we are neglecting diffusion of miRNA in the mRNA-rich region, the mRNA profile there is given by Eq. (4).

Microscopically, miRNA in the miRNA-rich zone diffuse in a landscape dominated by the linear decay channel leading to the decay length  $\lambda$  in Eq. (6). Upon entering the mRNA-rich region, where the nonlinear decay channel suddenly overwhelms the linear decay channel ( $km \gg \beta_\mu$ ), the miRNA are faced with an effective absorbing boundary. We therefore expect the miRNA concentration to vanish as one approaches the interface from the right. In addition, our picture asserts that the miRNA concentration is vanishingly small everywhere on the left of the interface. Taken together, these two properties impose zero miRNA concentration and zero miRNA flux at the interface. These two boundary conditions on the miRNA dynamics at the interface between mRNA-rich and miRNA-rich regions, together with the zero-flux condition at  $x = L$ , allow us to determine the position  $x_t$  of the interface. Furthermore, the interface must lie to the left of the crossing point of the transcription profiles,  $x_t < x_e$ , because the nonlinear channel for miRNA can only dominate when there is a reservoir of mRNA to annihilate with, i.e.  $\alpha_m > \alpha_\mu$ .

Armed with this insight into the miRNA profile we may now solve Eq. (5), subject to the boundary conditions  $-D\mu'(x_t) = -D\mu'(L) = 0$  and  $\mu(x_t) = 0$ , in terms of a Green's function. Making use of the zero-flux boundary conditions, the Green's function of Eq. (5) is

$$g(x, s) = \begin{cases} G(x, s) & \text{if } x < s \\ G(s, x) & \text{if } x > s \end{cases}, \quad (8)$$

where

$$\lambda G(x, s) = \frac{\cosh\left(\frac{x-x_t}{\lambda}\right) \cosh\left(\frac{L-s}{\lambda}\right)}{\sinh\left(\frac{L-x_t}{\lambda}\right)}. \quad (9)$$

The miRNA profile is then a weighted spatial average of the net transcriptional flux of miRNA to the right of the interface

$$\beta_\mu \mu(x) = \int_{x_t}^L [\alpha_\mu(s) - \alpha_m(s)] g(x, s) ds. \quad (10)$$

Employing the zero-concentration boundary condition  $\mu(x_t) = 0$ , we arrive at the following implicit equation for  $x_t$

$$\int_{x_t}^L [\alpha_\mu(s) - \alpha_m(s)] g(x_t, s) ds = 0. \quad (11)$$

Solving for  $x_t$  requires knowledge only of the transcription profiles. Moreover, one immediately sees that  $x_t$  can tolerate fluctuations in the transcription profiles which preserve the integral. This should be contrasted with  $x_e$  in the non-diffusive case which is less robust to small-number fluctuations.

In Figs. 1(c and d) we compare the analytical expressions in Eqs. (4), (10) and (11) with the exact numerical solution of Eqs. (2). As expected the agreement is good when the nonlinear channel dominates both the linear channel (Eq. (3)) and the diffusive channel ( $\ell \ll L$ ). The fact that the limits involve different parameters allows for a wide parameter regime where these conditions are met. One may try to reach these limits by sending  $\beta_m$  to zero. However, in this case, the source of mRNA ( $\alpha_m$ ) in the mRNA-rich zone would be larger than its sink ( $-\alpha_\mu$ ) and so steady state would never be reached. This is despite the fact that the total transcriptional flux of miRNA  $\int_0^L \alpha_\mu$  may be larger than that of mRNA. We conclude that the linear decay channel for mRNA must be open if the system is to sustain an interface at steady state.

### Generating a stripe

Using the insight gained in the previous section we briefly show how a stripe is formed when the miRNA transcription profile  $\alpha_\mu(x)$  is similar to  $\alpha_m(x)$  but displaced from it (Fig. 2(a)). An example occurs when the promoters of the miRNA and target have different affinities for a common regulator and different basal transcription rates. The transcription profiles cross at two points,  $x_{e1}$  and  $x_{e2} > x_{e1}$ . For low values of the annihilation rate  $k$  the miRNA and mRNA profiles (dotted lines, Fig. 2(b)) are qualitatively similar to their transcription profiles. As  $k$  is increased however miRNA deplete mRNA levels on the left and right of the developing field where  $\alpha_\mu > \alpha_m$  and thus confine mRNA expression to a stripe within the interval  $[x_{e1}, x_{e2}]$  (gray lines). Indeed, miRNAs which survive annihilation on the left and right diffuse into this interval and establish interfaces in the  $m$ -profile on the left at  $x_{t1}$  and on the right at  $x_{t2}$ . The location of these interfaces is determined analytically by solving Eq. (5) with zero-flux boundary conditions in the interval  $[0, x_{t1}]$  (and then enforcing  $\mu(x_{t1}) = 0$ ) and in the interval  $[x_{t2}, L]$  (and then enforcing  $\mu(x_{t2}) = 0$ ). In the region between the interfaces the mRNA profile is approximately given by  $m = [\alpha_m - \alpha_\mu]/\beta_m$ ; in the portion of the developing field complementary to this the mRNA profile is negligible. The analytic profiles for  $\mu$  and  $m$  are shown in black.

The effect on the interfaces of increased diffusion is two-fold and is illustrated in Fig. 2(c). The gray lines (exact numerical solutions for fixed  $k$ ) show that the interfaces become broader; the black lines (analytic solu-

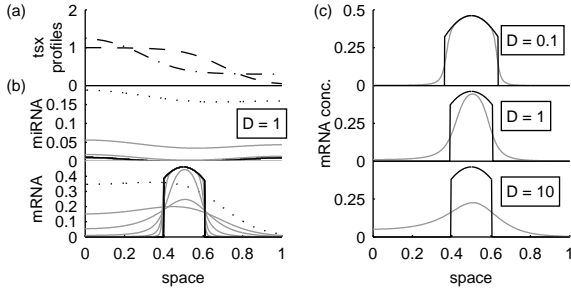


FIG. 2: Stripe generated by correspondent transcription profiles. (a) Correspondent transcription profiles of a miRNA (dashed-dotted) and its target (dashed), favorable for stripe generation. Such profiles occur, e.g., when the two species are regulated by a common regulator through similar but different promoters. Transcription profiles are the same as in Fig. 1, except that the miRNA transcription profile has been reflected about the center of the system and shifted upwards by 0.3. In addition the transcription profiles have been horizontally offset from one another:  $x_{tsx} = 0.3$  (miRNA) or 0.7 (mRNA). (b) miRNA and mRNA profiles for  $k = 10$  (dotted lines) and  $k = 10^2$  through  $10^6$  (gray lines). Analytic profiles in black. (c) The effect of diffusion constant  $D$  on mRNA profiles with  $k = 10^4$ . See caption of Fig. 1 for details.

tions) show that they also move closer to one another. To sustain a well-defined stripe of gene expression,  $\ell$ , which determines the interface width, must be much smaller than  $x_{e2} - x_{e1}$ .

### Possible experimental test

The model of morphogenetic regulation by miRNAs that we have presented possesses a distinct experimental signature that is visible in a genetic mosaic. We confine ourselves in this section to a pair of mutually exclusive transcription profiles. To illustrate the effect we consider first the limiting case where the mosaic consists of a single patch of cells that overexpress the miRNA (hereafter denoted the patch). The technique one uses to accomplish this may differ according to the stage of development under consideration. In the early blastoderm stages of *Drosophila* development, for example, a Gal4 driver may be used to drive expression of the miRNA in those cells where an endogenous gene is expressed [38]. Many endogenous genes are expressed in stripes along the anterior-posterior axis during these stages and some have dedicated enhancers for single stripes [4, 39]. In later stages of development, e.g. imaginal discs, a more natural technique is the random generation of mutant clones, at a low rate, by mitotic recombination [38, 40]. One then screens for those embryos containing a single clone. The patch has a qualitatively different effect depending on which side of the interface it occurs. These

effects should even be observable with digital experimental resolution where all fluorescence above an apparatus-dependent threshold is amplified to saturation.

Consider positioning the patch first in the miRNA-rich region of the developing field. We assume that the width  $w$  of the patch is of the order of a single cell (i.e.  $w \simeq L/100$ ). The patch increases the local miRNA transcription rate by an amount  $\alpha_c$ . We present results for patches positioned on the right of the mRNA interface in Fig. 3(a). One sees that, even if positioned at a distance from the expression domain of the target, the effect of the additional miRNA is to push the interface to a new position  $\hat{x}_t$ . The perturbation therefore, though introduced only locally, has a nonlocal effect.

We can understand this nonlocal effect with the aid of Eq. (5). By integrating this equation, and noting that the miRNA concentration is not much altered by the introduction of the patch (see Fig. 3(a)), one can show that

$$\alpha_c w \approx \int_{\hat{x}_t}^{x_t} \alpha_m. \quad (12)$$

Hence miRNA from the patch diffuse across the system towards the region  $[\hat{x}_t, x_t]$  and annihilate all mRNA produced there that would otherwise have maintained the interface at  $x_t$ .

This experiment should be contrasted with one in which the patch is positioned in the mRNA-rich region, as shown in Fig. 3(b). The effect of the perturbation is now a local one with excess miRNA creating a *hole* in the mRNA expression domain. The hole edges constitute two additional interfaces in the system, the sharpness of each again determined by  $\ell$ . The kinetics in this hole, where the miRNA transcription rate is large and the mRNA levels are low, is the same as those on the right of the original interface and so the width of the hole is given approximately by Eq. (12), where  $\hat{x}_t$  now represents the left edge of the hole and  $x_t$  represents the right edge.

We can make a quantitative testable prediction when there are a number of independent patches. To see this recall that Eq. (12) is an integral relationship. Hence the left-hand side is proportional to the number of patches, provided we make the reasonable assumption that the patches are uniform in size and transcription rate. Similarly, the right-hand side is proportional to the interface shift,  $x_t - \hat{x}_t$ , provided the mRNA transcription profile is sufficiently flat in the interval  $[\hat{x}_t, x_t]$ . Hence the interface position  $\hat{x}_t$  decreases linearly with the number of clones  $N$ . This prediction can readily be tested using an ensemble of embryos with varying numbers of clones.

The distinct nonlocal effect described above does not occur when the miRNA are unable to move between cells; in this case the excess miRNA are forced out of the system locally via the linear decay channel. Also, we have checked (for the parameters used in this study) that it does not occur when the miRNA acts purely enzymatically. Rather *both* miRNA mobility *and* a strong

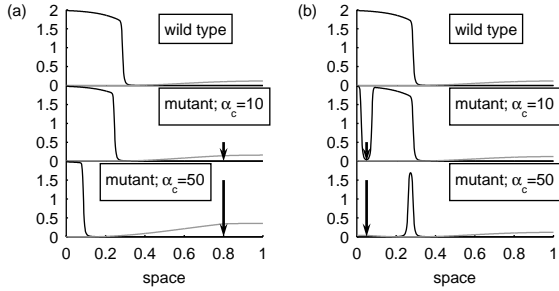


FIG. 3: The effect of a single miRNA-overexpressing patch on the mRNA profile. Throughout,  $\beta_m = 1$  and  $\beta_\mu = 1$ ,  $D = 1$ ,  $k = 10^5$  and  $w = 0.01$ . The unperturbed transcription profiles (upper portions of (a) and (b)) are as in Fig. 1. (a) A mutant clone in the miRNA-rich region (centered at  $x = 0.8$ ) pushes the interface to the left (lower two portions). (b) In contrast a mutant clone deep in the mRNA-rich region (centered at  $x = 0.05$ ) removes mRNA, producing a hole in the mRNA expression domain (lower two portions).

mutual annihilation between miRNA and target are required. The presence or absence of the nonlocal effect would therefore confirm or falsify the hypotheses that miRNA are mobile and that they interact stoichiometrically with mRNA while in this mobile state.

### Irreversible localization of miRNA

The situation where the transcription rates of miRNA and target are approximately equal in all cells may occur in the Hox gene network [20]. In the framework we have presented so far such a coincidence of transcription profiles would reduce steady-state mRNA (and miRNA) levels to negligible amounts in all cells. mRNA levels can, however, be rescued from global obliteration by extending the model to encompass the possibility that only those miRNA localized to a cell interact with their target. The target is rescued only if miRNA localization is irreversible; the case of rapid reversible localization reduces to the model studied in previous sections. We show in this section that this separation of diffusion and interaction permits the miRNA to perform the failsafe function described earlier, viz. low-abundance mRNA erroneously transcribed on the right of the developing field are cleared up by miRNA.

The separation of transport and interaction may occur in a number of ways. miRNA may be transported from cell to cell in a vessel that needs to be dismantled before miRNA can interact with mRNA. Alternatively, the interacting form of the RISC complex may be immobilized. Another possibility is that interaction between miRNA and mRNA is limited to specific loci in the cell, from which miRNA cannot escape. These scenarios—and others—are summarized by a model where miRNA ac-

quire a mobile state immediately after synthesis, and can switch into an interacting localized state at later times. This adds a new equation to our model which now takes the form

$$0 = \alpha - \beta_m m - k m \mu_l \quad (13a)$$

$$0 = q \mu - \beta_l \mu_l - k m \mu_l \quad (13b)$$

$$0 = \alpha - \beta_\mu \mu - q \mu + D \mu'' . \quad (13c)$$

Here  $\mu_l$  is the concentration of miRNA in the localized state, and  $q$  is an effective rate at which mobile miRNA switch into the interacting localized mode. The common transcription profiles of mobile miRNA and mRNA is denoted by  $\alpha(x)$ . The mobile-miRNA profile  $\mu(x)$  is determined only by the third equation and, by analogy with Eq. (10), is a weighted spatial average of  $\alpha$ . As such the effective transcription profile of immobile miRNA  $q\mu(x)$  is reduced on the left and increased on the right relative to that of the target  $\alpha(x)$  (compare dashed and dashed-dotted lines in Fig. 4). The first two equations then reduce to the zero-dimensional case considered earlier in which miRNA clear up mRNA to the right of the point where  $q\mu(x)$  and  $\alpha(x)$  cross (black line in Fig. 4).

The value of  $q$  which is most favorable for the failsafe function is  $q \approx \beta_\mu$ . To understand why it is helpful to consider two limits. In the first, the  $q$ -channel dominates all other loss channels for mobile miRNA, i.e.  $q \gg \beta_\mu$  and  $q \gg D/L^2$ . Hence all mobile miRNA immediately become immobile, the transcription profiles of mRNA and immobile miRNA coincide ( $\alpha \approx q\mu$ , Eq. ((13c))) and all mRNA are immediately annihilated in all cells. In the second limit, loss of mobile miRNA through the  $q$ -channel is negligible compared with the  $\beta_\mu$  channel,  $q \ll \beta_\mu$ , and very few mobile miRNA become immobile. Consequently  $\alpha \gg q\mu$  and there are practically no immobile miRNA available to affect the target. One measure of the efficacy of the failsafe mechanism is the ratio  $m(0)/m(L)$  which is plotted in Fig. 4(b) as a function of the localization rate  $q$ . One sees that the failsafe mechanism is most effective (represented by the largeness of the ratio  $m(0)/m(L)$ ) in the intermediate regime where  $q \approx \beta_\mu$ .

### DISCUSSION

In this study we have solved a model where miRNAs sharpen target gene expression patterns by generating an interface between high and low target expression. This cannot be achieved if the miRNA acts purely enzymatically nor can it be achieved if the miRNA does not move intercellularly. Such an interface can be directly detected provided the signal is not amplified to saturation and provided the threshold for detection is sufficiently low. One can in principle test the mutual-annihilation hypothesis by inhibiting the transcription of mRNA and monitoring its decay in time. The effective decay rate

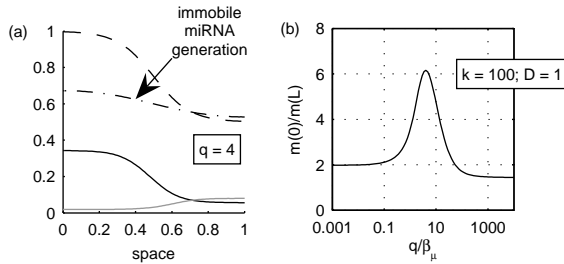


FIG. 4: Irreversible localization rescues the target from annihilation throughout the tissue and sharpens its expression pattern. (a) The effective transcription profile of the immobile miRNA  $q\mu(x)$  (dashed-dotted) is a broadened form of  $\alpha(x)$  (dashed). The mRNA profile (black line) exhibits a threshold response at the point where these two transcription profiles cross; miRNA profile is in gray. Other parameters are  $k = 100$  and  $D = 1$ . (b) The ratio between target expression at either end of the developing field is maximized when the localization rate  $q$  is in the vicinity of  $\beta_\mu$ .

$\beta_{eff}(t) = -\dot{m}(t)/m(t) = \beta_m + ks(t)$  is time-independent if the miRNA acts enzymatically and time-dependent if it acts stoichiometrically. We note also that a stoichiometric interaction may complicate the interpretation of sensor transgene experiments [20] as the transgene would then sequester miRNA and thereby alter the mRNA and original miRNA expression patterns.

The interface between low and high mRNA levels is characterized by low copy numbers of both RNA species. In such cases fluctuations in the copy number of either species may have macroscopic effects. For example, a small RNA-target pair in bacteria show enhanced fluctuations when their transcription rates become comparable [41, 42]. These fluctuations can in turn give rise to noise-induced bistability, which manifests itself experimentally as diversity in a population of cells [42]. We performed Monte-Carlo simulations of the model, but found that fluctuations have no macroscopic effect, even near the transition point where copy numbers of both species are low. This is because the interface position is determined by an integrated transcriptional flux (see Eq. (11)), which averages out individual cellular fluxes.

Candidate systems in which to test the ideas put forth in this study include the miR-165/7 system in plants [14, 15, 36] and the Hox system in mouse [20]. However the best system to study the sharpening of expression patterns is, arguably, the early *Drosophila* embryo. For example, though nuclei undergo rapid division cycles, the developing field does not change size, and so there is no need to incorporate growth into the patterning process.

Early embryonic development in *Drosophila* proceeds via a cascade of gene activities that progressively refine expression patterns along the anterior-posterior axis of the embryo. A recent study of the expression patterns

of nascent miRNA transcripts suggests that a number of miRNAs may play a role in this process. The miRNAs miR-309clus, miR-10 and iab-4 (which all reside between annotated mRNA genes on the genome), and miR-11, miR-274 and miR-281clus (which all reside within introns of annotated genes) are expressed in a graded fashion along the anterior-posterior axis of the blastoderm embryo [17, 43].

The complementary transcription profiles of iab-4 and its target Ubx at stage 5 [23] make this miRNA-target system a candidate for the sharpening mechanism proposed in this study. There is, however, a difficulty with this interpretation in that the system may not reach steady state before stage 6 when cells begin to migrate. In particular, no Ubx protein was detected at stage 5, possibly because of the time needed to transcribe the large Ubx locus [23]. The transcription profiles of iab-4 and Ubx at stage 5 do not seem to overlap [23], suggesting that iab-4 intercellular mobility may be crucial to allow it to interact with Ubx at this stage of development.

Like iab-4, the miRNA miR-10 is also expressed at stage 5 in a broad posterior region along the anterior-posterior axis [17]. The homeotic gene Scr is a predicted target of miR-10 [44] and is also expressed in the blastoderm at stage 5 [45]. The miR-10 site in the Scr 3'UTR is likely to be functional because the pairing is well conserved in all drosophilid genomes and because the miRNA site is conserved in the Scr genes in mosquito, the flour beetle and the silk moth [11]. Unlike Ubx, Scr protein is detected at this stage of development in a stripe of ectodermal cells about 4 cells wide in the parasegment-2 region, though it may not be functional at this time as the protein (a transcription factor) was not localized to the nucleus [45]. This spatial expression pattern is proximal to the anterior limit of miR-10 expression [17, 45]. Hence the interaction of miR-10 with Scr at stage 5 of *Drosophila* development is also a candidate for the sharpening mechanism.

The sharpening mechanism is most effective when the spatial transcription profiles of miRNA and target are regulated in such a way as to be mutually exclusive. The genomic locations of the miRNAs iab-4 and miR-10 are proximal to their targets consistent with the possibility of coordinated regulation [46].

It is a pleasure to thank William McGinnis, Martin F. Yanofsky and Jeffrey A. Long for useful discussions. This work has been supported in part by the NSF-sponsored Center for Theoretical Biological Physics (grant numbers PHY-0216576 and PHY-0225630).

---

[1] Driever, W & Nusslein-Volhard, C. (1988) *Cell* **54**, 83–93.  
[2] Driever, W & Nusslein-Volhard, C. (1988) *Cell* **54**, 95–

104.

[3] O'Connor, M. B, Umulis, D, Othmer, H. G, & Blair, S. S. (2006) *Development* **133**, 183–193.

[4] Janssens, H, Hou, S, Jaeger, J, Kim, H, Myasnikova, E, Sharp, D, & Reinitz, J. (2006) *Nature Gen.* **38**, 1159–1165.

[5] Lebrecht, D, Foehr, M, Smith, E, Lopes, F. J. P, Vanario-Alonso, C. E, Reinitz, J, Burz, D. S, & Hanes, S. D. (2005) *Proc. Natl. Acad. Sci.* **102**, 13176–13181.

[6] Melen, G. J, Levy, S, Barkai, N, & Shilo, B. Z. (2005) *Mol. Syst. Biol.* **1**, e1–e11.

[7] Kloosterman, W. P & Plasterk, R. H. A. (2006) *Developmental Cell* **11**, 441.

[8] Baulcombe, D. (2004) *Nature* **431**, 356.

[9] Bartel, D. P. (2004) *Cell* **116**, 281.

[10] Lewis, B. P, Burge, C. B, & Bartel, D. P. (2005) *Cell* **120**, 15.

[11] Brennecke, J, Stark, A, Russell, R. B, & Cohen, S. M. (2005) *PLoS Biol.* **3**, e85.

[12] Grün, D, Wang, Y. L, Langenberger, D, Gunsalus, K. C, & Rajewsky, N. (2005) *PLoS Comp. Biol.* **1**, e13.

[13] Chen, X. (2004) *Science* **303**, 2022.

[14] Juarez, M. T, Kui, J. S, Thomas, J, Heller, B. A, & Timmermans, M. C. P. (2004) *Nature* **428**, 84.

[15] Kidner, C. A & Martienssen, R. A. (2004) *Nature* **428**, 81.

[16] Valoczi, A, Varallyay, E, Kauppinen, S, Burgyan, J, & Havelda, Z. (2006) *The Plant J.* **47**, 140.

[17] Aboobaker, A. A, Tomancak, P, Patel, N, Rubin, G. M, & Lai, E. C. (2005) *Proc. Natl. Acad. Sci.* **102**, 18017.

[18] Biemar, F, Zinzen, R, Ronshaugen, M, Sementchenko, V, Manak, J. R, & Levine, M. S. (2005) *Proc. Natl. Acad. Sci.* **102**, 15907.

[19] Giraldez, A. J, Mishima, Y, Rihel, J, Grocock, R. J, Dongen, S. V, Inoue, K, Enright, A. J, & Schier, A. F. (2006) *Science* **312**, 75–79.

[20] Mansfield, J. H, Harfe, B. D, Nissen, R, Obenauer, J, Srineel, J, Chaudhuri, A, Farzan-Kashani, R, Zuker, M, Pasquinelli, A. E, Ruvkun, G, et al. (2004) *Nature Genetics* **36**, 1079.

[21] Hornstein, E & Shomron, N. (2006) *Nat. Gen. Supp.* **38**, S20.

[22] Hornstein, E, Mansfield, J. H, Yekta, S, Hu, J. K. H, Harfe, B. D, McManus, M. T, Baskerville, S, Bartel, D. P, & Tabin, C. J. (2005) *Nature* **438**, 671–674.

[23] Ronshaugen, M, Biemar, F, Piel, J, Levine, M, & Lai, E. C. (2005) *Genes & Dev.* **19**, 2947.

[24] Stark, A, Brennecke, J, Bushati, N, Russell, R. B, & Cohen, S. M. (2005) *Cell* **123**, 1133.

[25] Farh, K. K.-H, Grimson, A, Jan, C, Lewis, B. P, Johnston, W. K, Lim, L. P, Burge, C. B, & Bartel, D. P. (2005) *Science* **310**, 1817–1821.

[26] Sood, P, Krek, A, Zavolan, M, Macino, G, & Rajewsky, N. (2006) *Proc. Natl. Acad. Sci.* **103**, 2746.

[27] Zhao, Y, Samal, E, & Srivastava, D. (2005) *Nature* **436**, 214–20.

[28] O'Donnell, K. A, Wentzel, E. A, Zeller, K. I, Dang, C. V, & Mendell, J. T. (2005) *Nature* **435**, 839–43.

[29] Valencia-Sanchez, M. A, Liu, J, Hannon, G. J, & Parker, R. (2006) *Genes & Dev.* **20**, 515.

[30] Pillai, R. S, Bhattacharyya, S. N, & Filipowicz, W. (2007) *Trends Cell Biol.* in press.

[31] Haley, B & Zamore, P. D. (2004) *Nat Struct Mol Biol* **11**, 599–606.

[32] Liu, J, Valencia-Sanchez, M. A, Hannon, G. J, & Parker, R. (2005) *Nat. Cell. Biol.* **7**, 719.

[33] Levine, E, Levine, H, & Ben-Jacob, E. (2007). in preparation.

[34] Voinnet, O. (2005) *FEBS Letters* **579**, 5858.

[35] Yoo, B. C, Kragler, F, Varkonyi-Gasic, E, Haywood, V, Archer-Evans, S, Lee, Y. M, Lough, T. J, & Lucas, W. J. (2004) *Plant Cell* **16**, 1979.

[36] Emery, J, Floyd, S. K, Alvarez, J, Baum, S. F, & Bowman, J. L. (2003) *Curr. Biol.* **13**, 1768.

[37] Levine, E, Kuhlman, T, Zhang, Z, & Hwa, T. (2007). in preparation.

[38] Blair, S. S. (2003) *Development* **130**, 5065–5072.

[39] Small, S, Blair, A, & Levine, M. (1992) *EMBO J.* **11**, 4047–4057.

[40] Eldar, A & Barkai, N. (2005) *Dev. Biol.* **278**, 203–207.

[41] Elf, J, Paulsson, J, Berg, O. G, & Ehrenberg, M. (2003) *Biophys J* **84**, 154–70.

[42] Levine, E, Kuhlman, T, Zhang, Z, & Hwa, T. (2007). in preparation.

[43] Kosman, D, Mizutani, C. M, Lemons, D, Cox, W. G, McGinnis, W, & Bier, E. (2004) *Science* **305**, 846.

[44] Enright, A. J, John, B, Gaul, U, Tuschl, T, Sander, C, & Marks, D. S. (2003) *Genome Biol.* **5**, R1.

[45] Gorman, M. J & Kaufman, T. C. (1995) *Genetics* **140**, 557.

[46] Pearson, J. C, Lemons, D, & McGinnis, W. (2005) *Nature Reviews Gen.* **6**, 893.